Controlling single-emitter strong coupling by sculpting DNA dye scaffolds in NPoM cavities

Sara Rocchetti[1*], Thieme Schmidt[1], Ulrich F. Keyser[2*], Jeremy J. Baumberg[1*]

[1] Nanophotonics Centre, Cavendish Laboratory, University of Cambridge, Cambridge, CB3 0HE, UK
[2] Maxwell Centre, Cavendish Laboratory, University of Cambridge, Cambridge, CB3 0HE, UK
* email: ufk20@cam.ac.uk, jjb12@cam.ac.uk

Abstract

Coherent coupling of light and single-molecules enables the development of next-generation room-temperature-capable nanophotonics devices. Small mode-volume optical fields can be achieved with plasmonics, but challenges remain in placing oriented emitter molecules inside plasmonic cavities to access strong coupling consistently in emission. Using DNA origami, single-emitter molecules can be aligned inside sub-nanometric cavities created between a gold nanoparticle and gold mirror. We observe that the exact design of DNA scaffolding architecture surrounding a cyanine dye changes how its emission couples to the nanocavity, as well as how Au atoms respond to the optical forces, leading to continuous tuning of the dominant plasmonic mode. Through this, we show how strong coupling between three different dyes and the plasmon resonance always leads to low energy light emission, independent of detuning.

Keywords: *strong coupling, plasmonic, nanocavity, DNA origami, dye molecules*

Introduction

In recent years, the study of plasmon-exciton interactions at the single-molecule level has gained significant interest because of potential applications in enhancing optoelectronic devices, improving sensing technologies, and accessing quantum technologies at room temperature.[1] Creating strongly-coupled mixed states between individual emitters and visible light poses a significant challenge due to the hundred-fold difference in their spatial scales. This size mismatch is avoided by confining light inside deep sub-wavelength-sized nanocavities through exploiting metal plasmons, thereby achieving strong coupling.[2]

Accessing the single-molecule emission regime for strongly-coupled systems requires a substantial reduction in the typical number of molecules involved, and in combining robust precision placement with ultrasmall plasmonic optical volumes.[3] While self-assembled nanocavities can now routinely reduce optical mode volumes[4] (which parametrise the effective cavity round trip time for strong-coupling) below 100nm^3[3,5] further strategies to couple with a single ~nm^3 emitter are required to create systems that do not also damage under irradiation. To address this challenge, we use DNA nano-technology in conjunction with a nanoparticle-on-mirror (NPoM, **Fig. 1a,b**) geometry to explore how different dye molecules behave in such strong-coupling nanocavities. Recent advances in single

molecule confinement using DNA origami, have highlighted promising results through split peaks observed in light scattering[6–8]. However to date, the photoluminescence spectra from single emissive molecules in nanogaps have been somewhat inconsistent, hence the present study. We also note related work using single semiconductor colloidal quantum dots in plasmonic nanocavities,[9–12] which give rather different results to this corresponding single molecule emission, and highlight the possible differences from their much larger dipole size, isotropic dipole orientation, 3-fold degeneracy, and influence of a number of dark states.

We thus explore here how the precision and flexibility of DNA nanotechnology can avoid previous problems that led to gold facet destabilisation by using an alternative well-plate DNA-origami (DNAo) design. The provides excellent spatial alignment, which is critical for observing strong coupling, although we note orientational control of the emitter alignment is not yet solved. These well-plate scaffolded NPoM cavities are measured through dark-field (DF) scattering spectra that characterise the resulting architecture. The corresponding single-molecule photoluminescence (PL) spectra show strong-coupling for a variety of different detuning regimes using molecules with different emission energies, and reveal the influence on PL of mixing electronic states with the plasmon even for detunings > 0.5eV.

Methods

DNA origami folding and purification Single stranded viral DNA scaffold (7249 nucleotides) isolated from M13mp19 derivative is folded into rectangular DNA origami structures in 12 mM $MgCl_2$ and 1xTE buffer and purified from excess staples using centrifugal filtration. Further details on the folding and all experimental conditions for creating these structures can be found in our previous work.[13]

Gold nanoparticles functionalization and NPoM assembly AuNP (D=80 nm) are functionalised with an excess of single stranded DNA (thymine, 14 nucletoides) carrying a dithiol group on their 5' end side. The protocol is described in our previous work.[13] Purified DNA nanostructures (2 nM) are immobilised on a template-stripped gold film via their thiolated strands. A hydrophobic layer of dodecanethiol in ethanol (1 mM V/V) is used to passivate the free Au surface. DNA-functionalised AuNPs are then drop cast on the DNAo structures and let hybridise for at least 10 minutes, before being rinsed away.

Single nanoparticle DF and SERS measurements Both DF and SERS spectra are recorded on a home-built confocal Raman microscope. The setup features and details are described in our previous work.[13]

Results and Discussion

The well-plate DNA origami structure, designed with the software caDNAno, is comprised of 42 helices arranged in a double layer (**Fig. 1c,d**). Unlike previous rectangularly-shaped constructs which used a full double layer,[13] the central portion of the top layer is now removed to provide a 23x25 nm^2 aqueous well in proximity to the dye. For all details of the design and its assembly in solution and onto the Au, we refer the reader to our previous publication[13]. The excised scaffold is here shifted into unbound double helices lying outside the perimeter of the construct (**Fig. 1d**). The bottom layer of the DNAo is modified with thiolated strands (green in **c**), which bind the nanostructure onto a gold film via covalent bonds, and poly-adenine strands (blue in **c**), which capture poly-thymine coated

AuNPs (capture strands). Emitter molecules (purple in **c**) are bound at both their ends onto the lower layer but facing upwards, inside the central well. The 3D rendering of the final structure (**Fig. 1d**) is well matched by AFM images (**Fig. 1e**) confirming correct assembly of the DNAo structure, with homogeneous and well-separated constructs on the mica surface.

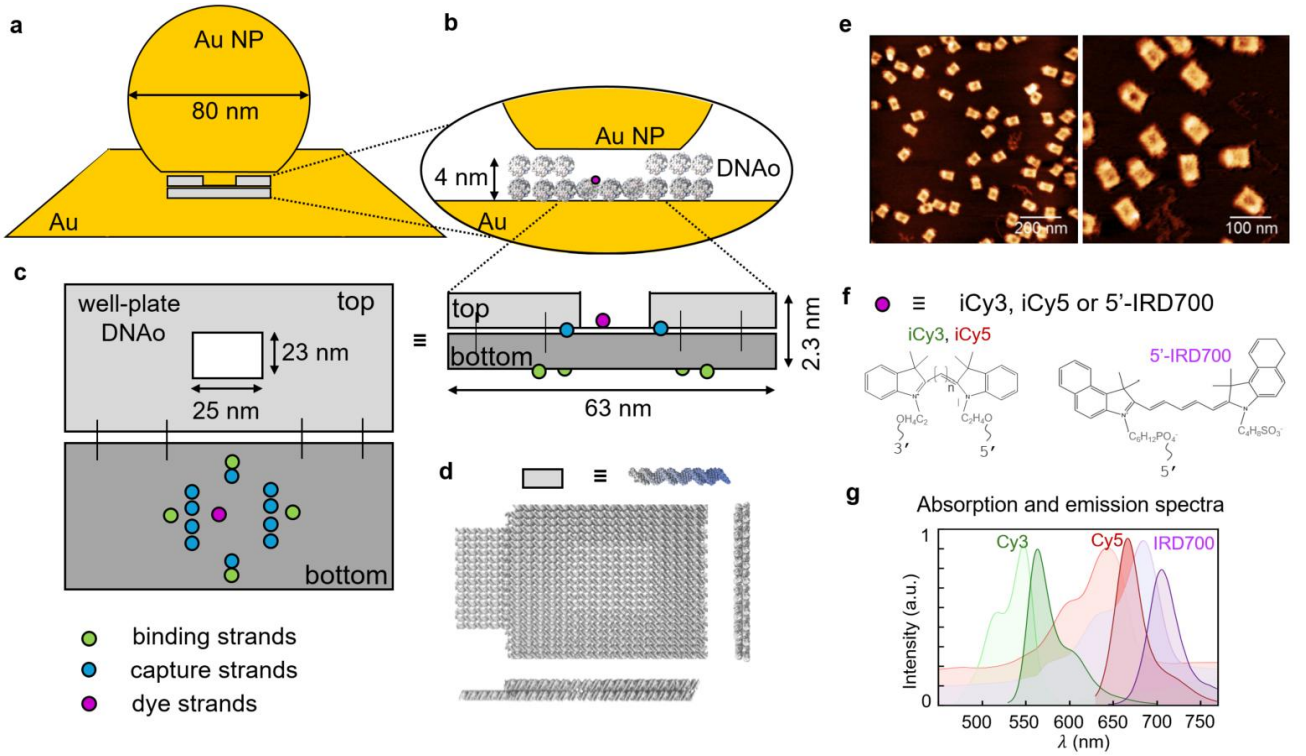

Fig. 1. Well-plate DNAo structure in nanoparticle-on-mirror (NPoM). a Schematic of well-plate DNAo scaffolding the nanogap of a NPoM cavity (not to scale). Inset in **b** shows the location of two single emitter sites (purple) on DNAo in the nanogap. **c** Bottom layer (dark-grey) of DNAo structure functionalised with binding strands (green) to allow immobilisation onto gold mirror, capture strands (blue) to fix AuNP onto the origami, and emitter binding strands (purple). **d** 3D rendering of final structure. **e** AFM images confirm the integrity of the DNA constructs on mica. **f** Molecular structures of internal cyanine dyes (iCy3, iCy5) and singly attached IRD700 dye (5'-IRD700). **g** Solution absorption (light shading) and fluorescence spectra (dark shading) of each dye.

Compared to previous studies using full-plates of DNAo, emitter molecules are now exposed to aqueous solution near the metal nanoparticle facet (**Fig. 1b**), rather than screened by Mg^{2+} ions bound to the phosphate backbone of DNA in between. This is found to enhance strong coupling interactions between the dye molecule (ω_X) and the confined cavity mode (ω_C). Here we compare three dyes (**Fig. 1f**) with different solution absorption/emission wavelengths (**Fig. 1g**) to investigate the influence of detuning $\Delta = \omega_X - \omega_C$. While the two cyanine dyes (Cy3 and Cy5) are linked as an internal modification on a single DNA strand which binds into the DNAo on both ends, the IRD700 dye has a single attachment from the 5'-end of a single DNA strand.

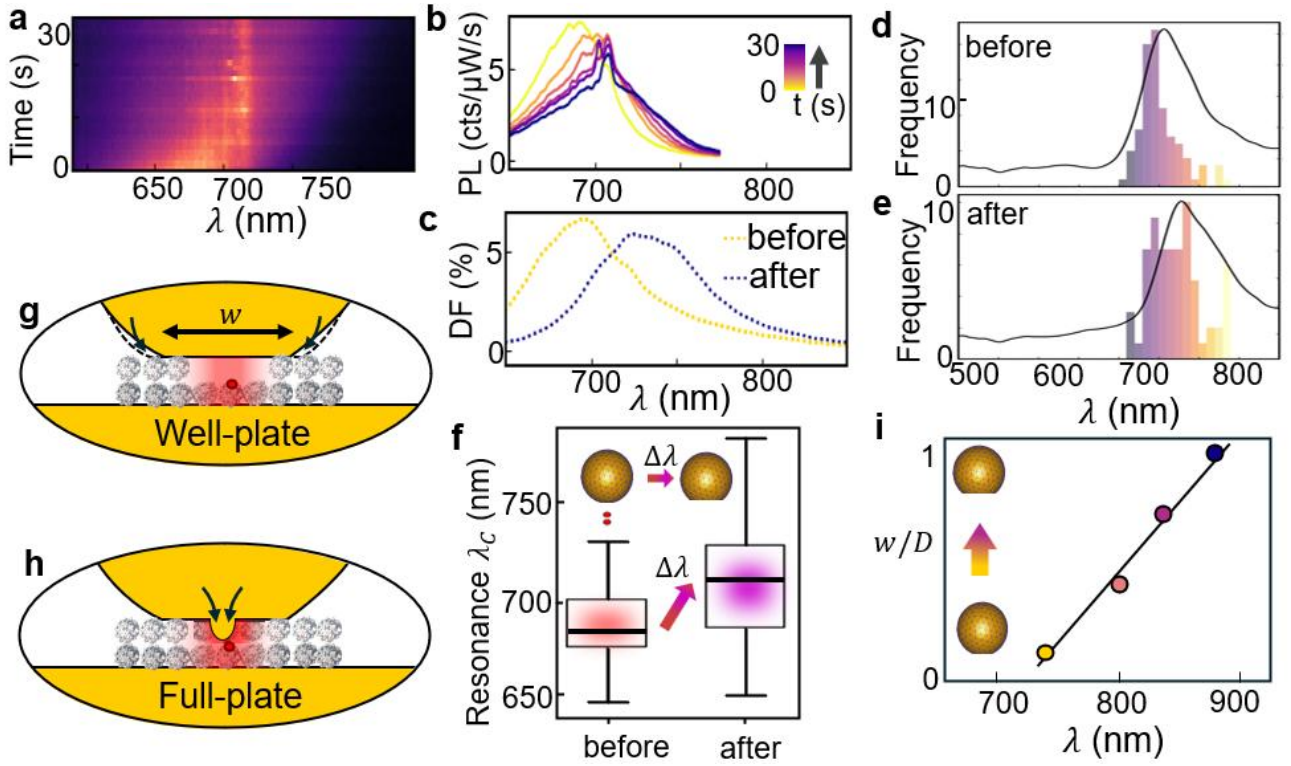

Fig. 2. a Evolution of emission with time from a single NPoM cavity containing a Cy5-labelled well-plate DNAo construct, pumped by $\lambda_p = 633$ nm laser light for 30 s. **b** Selected emission spectra shows gradual red-shift (yellow to purple = 0-30s) and increasingly intense Raman peaks ~690-710 nm. **c** Corresponding dark-field spectra before (yellow) and after (purple) laser illumination. **d**,**e** Histograms of DF resonant λ_C for >100 NPoMs before and after laser illumination, showing consistent red-shift in plasmon mode. Black curves are average DF spectra of mean bin. **f** Whisker boxplot of λ_C shows 35nm mean redshift (horizontal bars, arrow $\Delta\lambda$) after 30 s laser illumination. **g,h** Light-induced nanoparticle facet resculpting inferred for well-plate (g) and full-plate (h). **i** Simulated shifts from growth in facet size w (normalised by NP diameter D).

In previous studies,[5,13] we demonstrated the significant differences in emission properties of single dyes inside full-plate DNAo when in solution compared to when embedded in the NPoM geometry. However a significant unexpected feature was the enhanced light-induced instability of the facets. This arises because electronically resonant molecules generate large optical forces capable of extracting gold atoms from the nearby metallic surfaces.[14] This creation of chains of adatoms induces extremely strong new vibrational lines ('picocavities') which dominate the emission spectra, arising from surface-enhanced resonant-Raman signals (SERRS) from single dyes.[15]

Here by contrast, the well-plate DNAo nanogap spacer appears to produce much more gentle facet restructuring, comparable with previous experiments using robust MoS_2 and molecular monolayer spacers.[16,17] Emission (PL) spectra are collected using continuous illumination (λ_p = 633 nm, 150 μW.μm^{-2}) for 30 s (**Fig. 2a**). After background subtraction, the individual spectra show sharp Raman peaks together with a broad PL band which red-shifts over time (**Fig. 2b**). While initially the PL maximum is close to the solution Cy5 emission at 670 nm, it saturates around 710 nm, enhancing the Raman peaks (which match those from the dye and the adenine in DNA[18]) when it crosses them,

as expected from SERRS. To show these red-shifts are controlled by the plasmon resonance, we record dark-field scattering spectra before (yellow) and after (purple) laser illumination (**Fig. 2c**), which show a similar shift of the coupled mode $\Delta\lambda_C$.

To quantify this evolution of scattering peak position, we perform automated measurements on a large number of particles (>200 NPoMs), with the histogram of spectral peak positions generally shifting after illumination (**Fig. 2d**,**e**). Although both distributions are spread over σ_c=$\pm$30 nm, their mean position shifts by $\Delta\lambda_C \approx +35$ nm, as seen also in a whisker boxplot (**Fig. 2f**) of the average shifts.

The light-induced red-shifting of nanocavity plasmonic resonances has been observed in many experiments on such NPoM systems[16,17]. Its origin has been identified as arising from the restructuring of the lowest facet on near-spherical nanoparticles, and it is strongly retarded (or disappears) when the facet cannot restructure in this way, for instance using nanodecahedra with fixed (111) triangular facets[19], or nanocubes with fixed (100) square facets[16]. In neither case can the facets broaden in size due to the geometry of the nanoparticle, and indeed the light-induced red-shfting is now absent. This agrees with our previous work with DNA nanostructure-based NPoMs[13] which implied that these redshifts do not arise from compression of the nanogaps as water is expelled from the DNAo (as previously suggested[20]), because no difference is seen when our samples are immersed throughout in water. Similar shifts are also seen for completely incompressible 2D semiconductors in the nanogap.[17]

The cause of the red-shift is thus a slow migration of atoms around the side of the nanoparticle (due to a combination of strong light-induced van der Waals attraction which destabilises surface atoms and enhanced thermal diffusion). This increases the facet area (**Fig. 2g**), lowering the resonant energy of the system. This facet widening is rather different from the previous restructuring found with DNAo full-plates, as inferred from the picocavity SERRS (**Fig. 2h**), which suggested Au atoms were pulled right inside the DNAo structure.[13] The more gentle facet growth here saturates in time, due to the limiting wetting angle of the Au facet on the DNA set by the Au-DNA surface energy[17], as seen also for Au nano-dimers with thiol molecular spacers[21]. Nanocavity plasmon modes are sensitive to variations in the AuNP facet size,[16,22] allowing extraction of the cavity geometry by observing the coupled mode scattering positions.[19,22] We estimate the gap and facet size before and after laser illumination by comparing the scattering coupled mode peak position with previously published electrodynamics simulations,[22] which also includes details of these full electromagnetic simulations (that have been verified against experiments). These simulations imply an initial gap size of $\sim$4 nm, consistent with the double-layer DNA plate in the gap, and a facet diameter of w=(0.25$\pm$0.05)D, for spherical nanoparticle diameter D=80 nm. After laser illumination the gap is estimated to be $\sim$3 nm and facet size of (0.55$\pm$0.05)D, thus corresponding mainly to facet expansion. Simulated scattering spectra for nanoparticles with facets of increasingly-truncated spheres (**Fig. 2i**) reproduce these red-shifts.[23] We also note sporadic transient broad emission events (**Fig. 2a**), known as 'flares' that have

recently been identified as optical delamination of the top monolayer of Au atoms, and that may contribute to the slow atomic migration.[24]

In summary, we find here that removing DNA helices from the immediate vicinity of the dye molecule changes the type of optically-induced movement of Au atoms. When dsDNA surrounds the dye, the forces are sufficient to suck many Au atoms from the facet into its vicinity. On the other hand when there is pocket of water in the DNAo for the dye, these forces seem to be greatly reduced and only the typical facet widening is seen. However the cause of these differences is not yet clear. One possibility is that the polarizability of the solvated dye molecule can be reduced by ionic screening (even at optical frequencies), which in our models[14] would reduce the induced forces on the Au atoms. When DNA shrouds the dye this screening may not be possible (since the DNA binds the ions tightly). In the current situation, it shows the importance of the local environment of the dye (as in natural energy transfer cascades in rhodopsin, chlorophyll and other bio-photonic protein complexes[25]), which is accessed through DNAo design. This thus opens up a wealth of possibilities for further optimising chromophore-metal interactions in DNAo-scaffolded constructs.

We now explore the spectra that arise from emission of the dye molecule in this plasmonic environment. The slow tuning of the plasmon mode is extremely useful for examining the light-matter coupling since it allows (one-way) scanning of the detuning for each dye-plasmon construct (**Fig. 3**). Intriguingly, as the plasmon red-shifts from blue-detuning into resonance ($\Delta \sim 0$), a splitting in the scattering peak often appears (more than a third of the time). Differently from Fig.2c, in these cases an evident dark-field splitting is apparent by t=30s (purple), of magnitude $\Omega \sim 110$meV (**Fig. 3iii** dashed). Comparing the emission spectra (solid) also shows in this case a peak in-between the two split DF modes (partly masked by the strong SERRS peaks), also evident in **Fig. 3ii**. At t=0s however, this emission is slightly to the red side of the single DF peak observed (yellow curves), by on average 22nm across many NPoMs, which likely arises from the spectral separation between near-field and far-field resonances.[26]

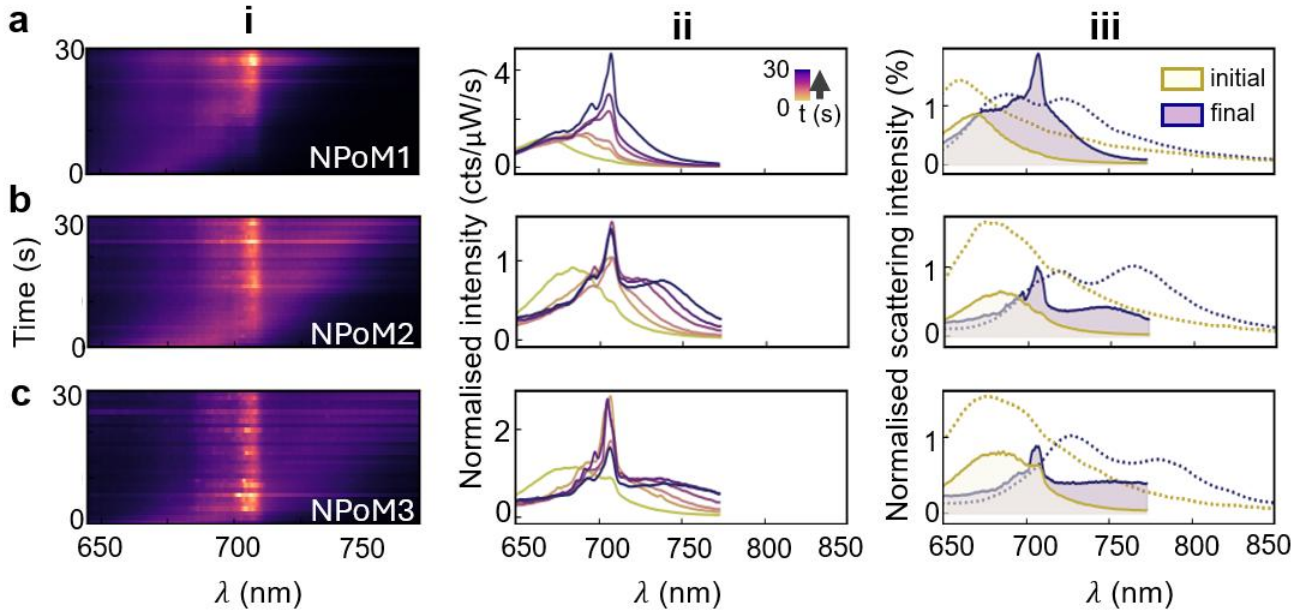

Fig. 3. a-c Emission from three NPoM cavities containing a single Cy5 emitter on the well-plate DNAo. **i,** Spectral maps, and **ii,** individual spectra over 30 s illumination. **iii,** Initial (yellow) and final (purple) spectra from emission (filled solid) and dark-field spectra (dotted), showing splitting in scattering spectra after red-shift of plasmon. The Raman peaks have here been fit and removed.

As shown in simulations below (based on proposals in [12,27]), these features are expected for the strong coupling regime when the linewidth Γ is comparable to the Rabi splitting Ω, because of the way that the DF and PL of the split polaritons interfere oppositely in the far-field. Illuminating through the cavity mode (for DF) produces destructive interference (hence partially cancelling to form a dip between $\omega_{\pm}$), while exciting non-resonantly via the exciton (for PL) gives constructive interference (obscuring the polariton splitting for $\Gamma \sim \Omega$ at $\Delta = 0$). The single-molecule Rabi splitting of Cy5 ($\sim$100meV with μ=0.9D)[28] observed here is three-fold smaller than that for methylene blue molecules ($\sim$300meV, μ=3.8D [5]), as expected from their relative transition dipole moments μ. However in the current realisation, precision of the number of dye molecules is ensured, making this a robust quantum emitting construct at room temperature. Besides gentle restructuring of the plasmonic facet (which saturates after $\sim$30s), the dye emission does not bleach, as previously noted because Purcell-enhanced re-emission is so fast in this NPoM that the molecule is vanishingly often found in the excited state.[29] The differences between these observations and previous experiments with larger gaps[6–8] (which show conventional quenching effects but do not evidence the spectral changes seen here) emphasises the effect of tighter confinement on the light-matter interactions.

For near zero detuning using Cy5 in these constructs, the Rabi coupling has to exceed the absorption linewidth and plasmon cavity linewidth for strong coupling.[30,31] In the intermediate regime here, splitting can be seen in DF but not in PL, however the real-time cavity retuning allows this to be verified for each construct. To further explore the strong coupling regime, we use the versatility of DNA nanotechnology to place differently detuned emitters inside the NPoM cavity, using Cy3 and IRD700 with emission wavelengths of 532 and 702 nm (**Fig. 1f**,**g**).

Despite their very different emission wavelengths, surprisingly strong emission is always observed in the vicinity of the resonant plasmon for these well-plate NPoM cavities (**Fig. 4**). For each molecule (a-c) we show exemplary spectra both initially (yellow) and after the facet growth has redshifted the plasmon (purple) for both PL emission (solid) and dark-field (dotted) spectra (**Fig. 4i**). Only for Cy5 is the strong coupling directly seen in DF after the plasmon tunes into resonance.

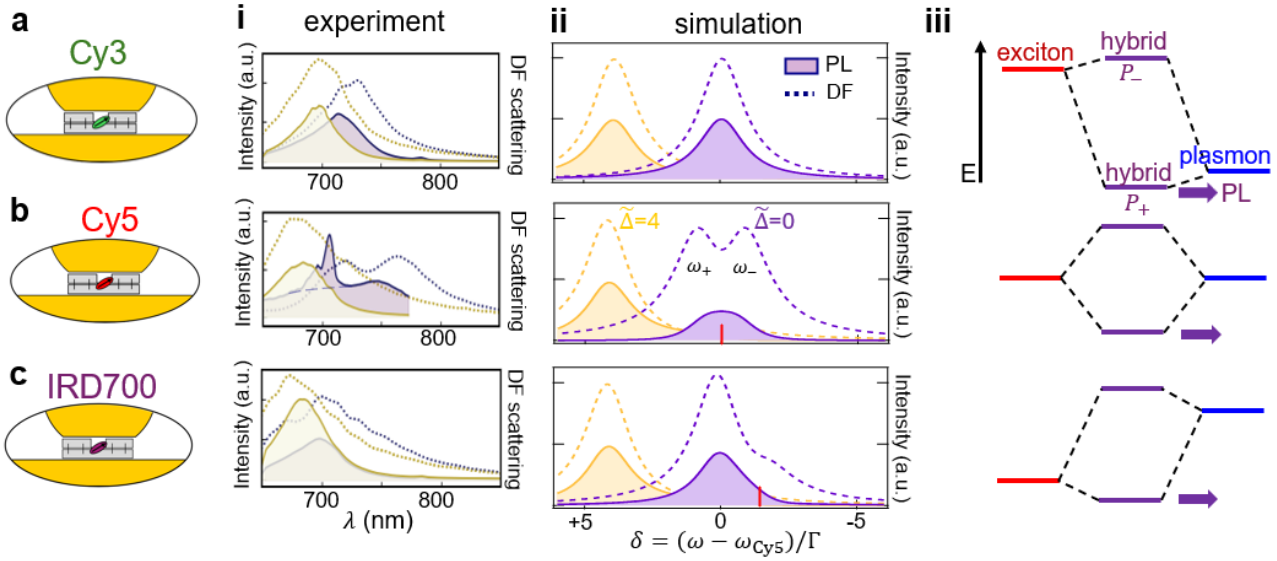

Figure 4. Comparing DNA origami NPoMs incorporating a single (**a**) Cy3, (**b**) Cy5, or (**c**) IRD700 molecule. **i,** Emission (solid) and dark-field (purple) spectra at t=0s (yellow) and t=30s (purple). Dashed line in **b,i** shows PL without SERRS peaks ~710 nm. **ii,** Simulations of dark-field and emission spectra at different normalised plasmon detunings $\tilde{\Delta} = (\omega_C - \omega_{Cy5})/\Gamma$, relative to the Cy5 transition (ω_{Cy5}). Transition dipoles 0.9,0.9,0.4D for a-c. **iii,** Energy level diagram showing exciton and plasmon energies for each emitter-plasmon pair.

To tentatively understand why non-resonant molecules emit at the plasmon wavelength, we consider the strongly-coupled plexciton (hybrid plasmon-exciton) for the parameters of our experiment. Using the standard strong-coupling Hopfield model[32] gives simulated spectra which match the experimental data reasonably well (**Fig. 4ii**). In this picture the reason why that despite its larger detuning, the Cy3 still emits strongly is due to the hybridisation of the exciton with the plasmon (**Fig. 4iii**). Despite a small energy shift in the lower plexciton P_+, the mixing in of the exciton component allows efficient emission of this quasiparticle (purple arrows). In all cases, emission to the lower polariton (plexciton) state is rapid, so that it domaintes absorption and emission.

Only for the resonant detuning case with Cy5, is intense SERRS observed, which is maximised for $\tilde{\Delta}$=0. In this case the branching ratio between PL and SERRS becomes near-unity, showing that relaxation within the excited electronic vibrational manifold can be slower than photon emission via plexcitons to the ground state vibrational manifold. In all other cases, Kasha's rule is observed and non-resonant SERS is too weak to be seen. It is also apparent that the plasmon shifts are stronger for the resonant Cy5 molecule than the weaker-coupled Cy3 and IRD700, confirming that resculpting of the Au facet depends on the resonant polarisability of the single molecule inside the nanogap.

Finally we note the important effects of dye dipole orientation in such nanogaps. The optical field perpendicular to the metal is more than ten-fold stronger than the in-plane fields at the position of the dye. This means that in-plane dipole orientations would not emit light, while perpendicular orientations are needed for strong light-matter coupling. Here the Cy3,5 dyes are tethered into the structure at both oligo ends, but the IR700 is only bound from one end (Fig.1), however no clear difference in signatures are seen. For instance their dynamics are similar, without any signature of rapid reorientations that might be expected for the IR700 as it diffuses around in the water pocket inside the DNAo. We thus cannot conclude anything here about orientation, although it remains an interesting question for future work.

We also note that previous (relatively) simple theoretical models for strong coupling may not be applicable here. The very large electron density in the Au facets is situated less that then the dipole size away, and thus can have much more profound changes on the emission spectrum. The dipole-dipole interactions from electron wavepackets in the emitting dye molecule and screening electrons in the metal (as well as the high-density ions solvated in the water pocket) can have a profound effect on all processes including Rayleigh and Raman scattering, non-radiative absorption, energy relaxation within the molecule and phonon-interactions, as well as the fundamental emission process which operates in optical field gradients that can now be on the scale of the emitting dipole. We thus emphasize the need for further developments, using these precision nanoassembly techniques.

Conclusions

In conclusion, we show that DNA origami architectures change the electromagnetic interactions of dye molecules and Au facets, as well as the light-matter coupling. The presence of water solvating the dye leads to different optical-induced forces, which we suggest arises from the local screening of the optical dipole. We show a design of well-plate scaffolded NPoM cavities which appear to give strong coupling effects from single molecule emitters and plasmonic modes, experimentally observed as a peak splitting in the cavity dark-field spectrum. When detuned from the plasmon energy, emitters in these plasmonic cavities couple only weakly with the cavity, but give significant emission at the lower polariton energy due to hybridisation. The versatility of DNA nanotechnology thus opens up a myriad of possibilities in the field of quantum technology and nanophotonics information.

Author information

Corresponding authors

Jeremy Baumberg: jjb12@cam.ac.uk

Ulrich Keyser: ufk20@cam.ac.uk

Author contributions

S.R. and J.J.B. conceived and designed the experiments. S.R., T.S. and U.F.K. designed and optimized the DNA origami structures. S.R. carried out the optical experiments, and analysed the data together with J.J.B. All authors contributed to the manuscript writing and/or editing.

Data availability

All data needed to evaluate the conclusions in the paper are present in the paper.

Competing interests

The authors declare no competing interests.

Acknowledgements

We thank support from UK EPSRC EP/X037770/1, and the European Research Council (ERC) under the Horizon 2020 Research and Innovation Programme PICOFORCE (883703).

TOC graphic

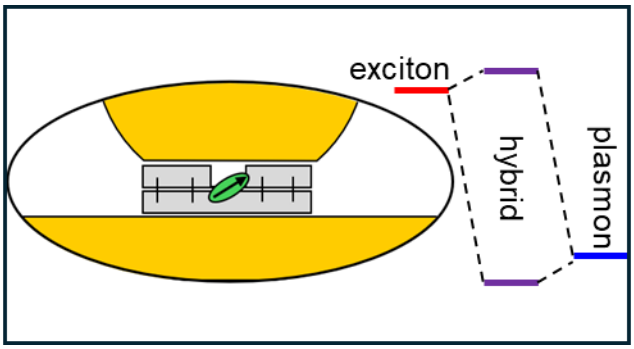

References

(1) Dovzhenko, D. S.; Ryabchuk, S. V.; Rakovich, Y. P.; Nabiev, I. R. Light-Matter Interaction in the Strong Coupling Regime: Configurations, Conditions, and Applications. *Nanoscale* **2018**, *10*, 3589–3605. https://doi.org/10.1039/c7nr06917k.

(2) Rodriguez, S. R.-K. Classical and Quantum Distinctions between Weak and Strong Coupling. *Eur. J. Phys.* **2016**, *37* (2), 025802. https://doi.org/10.1088/0143-0807/37/2/025802.

(3) Kongsuwan, N.; Demetriadou, A.; Chikkaraddy, R.; Benz, F.; Turek, V. A.; Keyser, U. F.; Baumberg, J. J.; Hess, O. Suppressed Quenching and Strong-Coupling of Purcell-Enhanced Single-Molecule Emission in Plasmonic Nanocavities. *ACS Photonics* **2018**, *5* (1), 186–191. https://doi.org/10.1021/acsphotonics.7b00668.

(4) Huang, S.; Ming, T.; Lin, Y.; Ling, X.; Ruan, Q.; Palacios, T.; Wang, J.; Dresselhaus, M.; Kong, J. Ultrasmall Mode Volumes in Plasmonic Cavities of Nanoparticle-On-Mirror Structures. *Small* **2016**, *12* (37), 5190–5199. https://doi.org/10.1002/smll.201601318.

(5) Chikkaraddy, R.; De Nijs, B.; Benz, F.; Barrow, S. J.; Scherman, O. A.; Rosta, E.; Demetriadou, A.; Fox, P.; Hess, O.; Baumberg, J. J. Single-Molecule Strong Coupling at Room Temperature in Plasmonic Nanocavities. *Nature* **2016**, *535* (7610), 127–130. https://doi.org/10.1038/nature17974.

(6) Kaminska, I.; Bohlen, J.; Mackowski, S.; Tinnefeld, P.; Acuna, G. P. Strong Plasmonic Enhancement of a Single Peridinin–Chlorophyll *a* –Protein Complex on DNA Origami-Based

Optical Antennas. *ACS Nano* **2018**, *12* (2), 1650–1655. https://doi.org/10.1021/acsnano.7b08233.
(7) Yeşilyurt, A. T. M.; Huang, J. Emission Manipulation by DNA Origami-Assisted Plasmonic Nanoantennas. *Adv. Opt. Mater.* **2021**, *9* (21), 2100848. https://doi.org/10.1002/adom.202100848.
(8) Roller, E.-M.; Argyropoulos, C.; Högele, A.; Liedl, T.; Pilo-Pais, M. Plasmon–Exciton Coupling Using DNA Templates. *Nano Lett.* **2016**, *16* (9), 5962–5966. https://doi.org/10.1021/acs.nanolett.6b03015.
(9) Park, K.-D.; May, M. A.; Leng, H.; Wang, J.; Kropp, J. A.; Gougousi, T.; Pelton, M.; Raschke, M. B. Tip-Enhanced Strong Coupling Spectroscopy, Imaging, and Control of a Single Quantum Emitter. *Sci. Adv.* **2019**, *5* (7), eaav5931. https://doi.org/10.1126/sciadv.aav5931.
(10) Santhosh, K.; Bitton, O.; Chuntonov, L.; Haran, G. Vacuum Rabi Splitting in a Plasmonic Cavity at the Single Quantum Emitter Limit. *Nat. Commun.* **2016**, *7* (1), ncomms11823. https://doi.org/10.1038/ncomms11823.
(11) Groß, H.; Hamm, J. M.; Tufarelli, T.; Hess, O.; Hecht, B. Near-Field Strong Coupling of Single Quantum Dots. *Sci. Adv.* **2018**, *4* (3), eaar4906. https://doi.org/10.1126/sciadv.aar4906.
(12) Hu, S.; Huang, J.; Arul, R.; Sánchez-Iglesias, A.; Xiong, Y.; Liz-Marzán, L. M.; Baumberg, J. J. Robust Consistent Single Quantum Dot Strong Coupling in Plasmonic Nanocavities. *Nat. Commun.* **2024**, *15* (1), 6835. https://doi.org/10.1038/s41467-024-51170-7.
(13) Rocchetti, S.; Ohmann, A.; Chikkaraddy, R.; Kang, G.; Keyser, U. F.; Baumberg, J. J. Amplified Plasmonic Forces from DNA Origami-Scaffolded Single Dyes in Nanogaps. *Nano Lett.* **2023**, *23* (13), 5959–5966. https://doi.org/10.1021/acs.nanolett.3c01016.
(14) Lin, Q.; Hu, S.; Földes, T.; Huang, J.; Wright, D.; Griffiths, J.; Elliott, E.; De Nijs, B.; Rosta, E.; Baumberg, J. J. Optical Suppression of Energy Barriers in Single Molecule-Metal Binding. *Sci. Adv.* **2022**, *8* (25), eabp9285. https://doi.org/10.1126/sciadv.abp9285.
(15) Biaggne, A.; Kim, Y. C.; Melinger, Joseph. S.; Knowlton, W. B.; Yurke, B.; Li, L. Molecular Dynamics Simulations of Cyanine Dimers Attached to DNA Holliday Junctions. *RSC Adv.* **2022**, *12* (43), 28063–28078. https://doi.org/10.1039/D2RA05045E.
(16) Xomalis, A.; Chikkaraddy, R.; Oksenberg, E.; Shlesinger, I.; Huang, J.; Garnett, E. C.; Koenderink, A. F.; Baumberg, J. J. Controlling Optically Driven Atomic Migration Using Crystal-Facet Control in Plasmonic Nanocavities. *ACS Nano* **2020**, *14* (8), 10562–10568. https://doi.org/10.1021/acsnano.0c04600.
(17) Mertens, J.; Demetriadou, A.; Bowman, R. W.; Benz, F.; Kleemann, M.-E.; Tserkezis, C.; Shi, Y.; Yang, H. Y.; Hess, O.; Aizpurua, J.; Baumberg, J. J. Tracking Optical Welding through Groove Modes in Plasmonic Nanocavities. *Nano Lett.* **2016**, *16* (9), 5605–5611. https://doi.org/10.1021/acs.nanolett.6b02164.
(18) Safar, W.; Azziz, A.; Edely, M.; Lamy De La Chapelle, M. Conventional Raman, SERS and TERS Studies of DNA Compounds. *Chemosensors* **2023**, *11* (7), 399. https://doi.org/10.3390/chemosensors11070399.
(19) Hu, S.; Elliott, E.; Sánchez-Iglesias, A.; Huang, J.; Guo, C.; Hou, Y.; Kamp, M.; Goerlitzer, E. S. A.; Bedingfield, K.; De Nijs, B.; Peng, J.; Demetriadou, A.; Liz-Marzán, L. M.; Baumberg, J. J. Full Control of Plasmonic Nanocavities Using Gold Decahedra-on-Mirror Constructs with Monodisperse Facets. *Adv. Sci.* **2023**, *10* (11), 2207178. https://doi.org/10.1002/advs.202207178.
(20) Simoncelli, S.; Roller, E.-M.; Urban, P.; Schreiber, R.; Turberfield, A. J.; Liedl, T.; Lohmüller, T. Quantitative Single-Molecule Surface-Enhanced Raman Scattering by Optothermal Tuning of

DNA Origami-Assembled Plasmonic Nanoantennas. *ACS Nano* **2016**, *10* (11), 9809–9815. https://doi.org/10.1021/acsnano.6b05276.
(21) Salmon, A. R.; Kleemann, M.-E.; Huang, J.; Deacon, W. M.; Carnegie, C.; Kamp, M.; De Nijs, B.; Demetriadou, A.; Baumberg, J. J. Light-Induced Coalescence of Plasmonic Dimers and Clusters. *ACS Nano* **2020**, *14* (4), 4982–4987. https://doi.org/10.1021/acsnano.0c01213.
(22) Elliott, E.; Bedingfield, K.; Huang, J.; Hu, S.; De Nijs, B.; Demetriadou, A.; Baumberg, J. J. Fingerprinting the Hidden Facets of Plasmonic Nanocavities. *ACS Photonics* **2022**, *9* (8), 2643–2651. https://doi.org/10.1021/acsphotonics.2c00116.
(23) Guo, C.; Benzie, P.; Hu, S.; De Nijs, B.; Miele, E.; Elliott, E.; Arul, R.; Benjamin, H.; Dziechciarczyk, G.; Rao, R. R.; Ryan, M. P.; Baumberg, J. J. Extensive Photochemical Restructuring of Molecule-Metal Surfaces under Room Light. *Nat. Commun.* **2024**, *15* (1), 1928. https://doi.org/10.1038/s41467-024-46125-x.
(24) Baumberg, J. J. Quantum Plasmonics in Sub-Atom-Thick Optical Slots. *Nano Lett* **2023**, *23*, 10696–10702.
(25) De Grip, W. J.; Ganapathy, S. Rhodopsins: An Excitingly Versatile Protein Species for Research, Development and Creative Engineering. *Front. Chem.* **2022**, *10*, 879609. https://doi.org/10.3389/fchem.2022.879609.
(26) Lombardi, A.; Demetriadou, A.; Weller, L.; Andrae, P.; Benz, F.; Chikkaraddy, R.; Aizpurua, J.; Baumberg, J. J. Anomalous Spectral Shift of Near- and Far-Field Plasmonic Resonances in Nanogaps. *ACS Photonics* **2016**, *3* (3), 471–477. https://doi.org/10.1021/acsphotonics.5b00707.
(27) Leng, H.; Szychowski, B.; Daniel, M.-C.; Pelton, M. Strong Coupling and Induced Transparency at Room Temperature with Single Quantum Dots and Gap Plasmons. *Nat. Commun.* **2018**, *9* (1), 4012. https://doi.org/10.1038/s41467-018-06450-4.
(28) Bamgbelu, A.; Wang, J.; Leszczynski, J. TDDFT Study of the Optical Properties of Cy5 and Its Derivatives. *J. Phys. Chem. A* **2010**, *114*, 3551–3555.
(29) Horton, M. J.; Ojambati, O. S.; Chikkaraddy, R.; Deacon, W. M.; Kongsuwan, N.; Demetriadou, A.; Hess, O.; Baumberg, J. J. Nanoscopy through a Plasmonic Nanolens. *Proc. Natl. Acad. Sci.* **2020**, *117* (5), 2275–2281. https://doi.org/10.1073/pnas.1914713117.
(30) Heintz, J.; Markešević, N.; Gayet, E. Y.; Bonod, N.; Bidault, S. Few-Molecule Strong Coupling with Dimers of Plasmonic Nanoparticles Assembled on DNA. *ACS Nano* **2021**, *15*, 14732–14743.
(31) Koch, J.; Hunanyan, G. R.; Ockenfels, T.; Rico, E.; Solano, E.; Weitz, M. Quantum Rabi Dynamics of Trapped Atoms Far in the Deep Strong Coupling Regime. *Nat. Commun.* **2023**, *14* (1), 954. https://doi.org/10.1038/s41467-023-36611-z.
(32) Kavokin, A. V.; Baumberg, J.; Malpuech, G.; Laussy, F. P. *Microcavities*, Second edition.; Series on semiconductor science and technology; Oxford University Press: Oxford, 2017.